Eur. Phys. J. Special Topics **226**, 1939–1951 (2017)

DOI: 10.1140/epjst/e2017-70024-6

THE EUROPEAN PHYSICAL JOURNAL SPECIAL TOPICS

Regular Article

A critical firing rate associated with tonic-to-bursting transitions in synchronized gap-junction coupled neurons

Annabelle Shaffer[1], Rosangela Follmann[2,1], Allison L. Harris[1], Svetlana Postnova[3], Hans Braun[4], and Epaminondas Rosa, Jr.[1,2,a]

[1] Department of Physics, Illinois State University, Normal, IL 61790, USA
[2] School of Biological Sciences, Illinois State University, Normal, IL 61790, USA
[3] School of Physics, University of Sydney, New South Wales, Sydney, Australia
[4] Institute of Physiology, University of Marburg, 35037 Marburg, Germany

Received 31 January 2017 / Received in final form 9 March 2017
Published online 21 June 2017

Abstract. A transition between tonic and bursting neuronal behaviors is studied using a linear chain of three electrically coupled model neurons. Numerical simulations show that, depending on their individual dynamical states, the neurons first synchronize either in a tonic or in a bursting regime. Additionally, a characteristic firing rate, mediating tonic-to-bursting transitions in networked neurons, is found to be associated with a firing rate encountered in the single neuron's equivalent transition. A few cases describing this peculiar phenomenon are presented.

1 Introduction

Coordinated neuronal network activity, particularly synchronous, is vital for the survival of many organisms. Synchrony in neurons is known to be of relevance in a number of processes including learning and memory [1–3], wake-sleep cycles [4,5], central pattern generators [6], and neurological conditions such as epilepsy [7,8] and Parkinson's disease [9].

In this study we describe a tonic (rhythmic single spiking) to bursting (repeating sequences of multiple spikes) transition taking place in triads of synchronous model neurons connected via electrical synapses. Electrical synapses are channel-shaped structures formed in contacting membranes of nerve cells enabling electrical transmission between them. This type of synapses between neurons was demonstrated in the pioneer work of Furshpan and Potter [10], and its role in neuronal communication has since become better understood and appreciated [11]. Additionally, electrical synapses are known to promote synchrony in networked neurons [12], and are believed to have decisive roles in seizures [13] and in pattern formation and development [14]. Our network model involves three distinct neurons (one tonic and two bursting) reciprocally coupled via electrical synapses in a linear chain format. The center neuron

[a] e-mail: erosa@ilstu.edu

(neuron 1) and the two outer neurons (neurons 0 and 2) have identical but variable couplings, i.e., $g_{c01} = g_{c12} = g_c$ is a control parameter defining the strength of the connections between the neurons. Neuron 1 can be viewed as a relay neuron, allowing neurons 0 and 2 communicate with each other.

Also known as interneurons, relay neurons are not uncommon, carrying information from one part of the central nervous system to another, and being of major relevance in neuronal communication. For example, thalamocortical cells performing sensory, motor or a higher order associational role are subject to switching modes of responsiveness that are elicited by relay neurons. Recent fMRI and physiology studies indicate that perceptual and cognitive tasks modulate responses in the visual thalamus [15], suggesting that the thalamus does more than just the passive relaying of sensory information to the cortex [16].

Furthermore, some neuronal synchronous states are directly related to transitions between tonic and bursting activity, including arrays of noisy neurons [17]. Tonic-to-bursting transitions are important, for example, in thalamocortical neurons at sleeping transition states [18], and in sensory-motor nuclei producing tremors in Parkinson's disease [19]. Transitions of this nature have been investigated, mostly involving the dynamics of individual neurons [20,21], and not much is known about these transitions involving distinct coupled neurons.

Here we focus on the tonic-to-bursting transition taking place in triads of coupled synchronous model neurons. Our results indicate that the typical tonic-to-bursting transition encountered in the single neuron model is carried over to the network of neurons in a peculiar way. The single neuron undergoes this transition for a particular value of its slow repolarization conductance, $g_{sr}^{critical} = 0.305\,\mathrm{mS/cm^2}$, with a particular firing rate $f^{critical} = 1.25\,\mathrm{Hz}$. The three-neuron network we study undergoes an equivalent transition, with a variety of different g_{sr} values for the individual neurons, but firing together at the common firing rate $f^{critical} = 1.25\,\mathrm{Hz}$. In the network, the transition happens when the synchronous neurons undergo their first period-doubling bifurcation en route to chaos and then to bursting, creating a clear separation between tonic and bursting synchronous states. However, while the tonic-to-bursting transition in synchronous neurons is mediated by a period-doubling cascade and chaos [22], the equivalent transition for the single neuron is followed by a period-adding sequence [23].

2 Model equations

The Huber-Braun model equations used for representing the neuron in this work are a variation of the Hodgkin and Huxley model [24], include physiologically relevant components, and have been widely applied to a number of situations [25–30]. Briefly, the Huber-Braun equations consist of a set of four differential equations (one for the voltage and three for electric current activation functions) describing the dynamics of ionic flows across the cell's membrane.

The equation for the membrane voltage of neuron (j) coupled to two other neurons (i and k) is given by

$$C\dot{V}_{\mathrm{j}} = -I_{\mathrm{leak}} - I_{\mathrm{Na}} - I_{\mathrm{K}} - I_{\mathrm{sd}} - I_{\mathrm{sr}} - I_{\mathrm{inj}} - I_{\mathrm{ji}} - I_{\mathrm{jk}}. \tag{1}$$

Here C represents the membrane capacitance, the leak current is given by $I_{\mathrm{leak}} = g_{\mathrm{leak}}(V - V_{0\mathrm{leak}})$ where g_{leak} is the leak conductance (constant) and $V_{0\mathrm{leak}}$ is the equilibrium potential. The fast currents for sodium I_{Na} and potassium I_{K} are accompanied by the corresponding slow depolarization sodium current I_{sd} and the slow repolarization potassium calcium-dependent current I_{sr}. The maximum conductances and equilibrium potentials are represented by g_{q} and $V_{0\mathrm{q}}$, respectively. I_{inj} denotes a

constant current injection, and the terms I_{ji} and I_{jk} represent the coupling currents between the pairs of neurons.

The opening and closing of the ion channels are directly associated with characteristic time constants τ_{q}. For the fast income of sodium the activation function is given by $a_{\mathrm{Na}} = \frac{1}{1+e^{-s_{\mathrm{Na}}(V-V_{0_{\mathrm{Na}}})}}$, where s_{Na} represents the slope of the sigmoid curve, and $V_{0_{\mathrm{Na}}}$ corresponds to the half-activation potential. For fast potassium activation, slow sodium activation and slow potassium activation, the equations are, respectively

$$\dot{a}_{\mathrm{K}} = \frac{\phi}{\tau_{\mathrm{K}}}(a_{\mathrm{K}\infty} - a_{\mathrm{K}}), \tag{2}$$

$$\dot{a}_{\mathrm{sd}} = \frac{\phi}{\tau_{\mathrm{sd}}}(a_{\mathrm{sd}\infty} - a_{\mathrm{sd}}), \tag{3}$$

$$\dot{a}_{\mathrm{sr}} = -\frac{\phi}{\tau_{\mathrm{sr}}}(\nu_{\mathrm{acc}} I_{\mathrm{sd}} + \nu_{\mathrm{dep}} a_{\mathrm{sr}}). \tag{4}$$

The scaling parameters for temperature dependencies are $\rho = 0.607$ and $\phi = 0.124$. Equations (2)–(4) represent the activation functions for potassium, slow depolarization, and slow repolarization, respectively. The activation functions $a_{\mathrm{q}\infty}$ are represented by sigmoid steady state curves given by $a_{\mathrm{q}\infty} = \frac{1}{1+e^{-s_{\mathrm{q}}(V-V_{0\mathrm{q}})}}$, q = K, sd, sr. In this model $a_{\mathrm{Na}} \equiv a_{\mathrm{Na}\infty}$, as a result of the very fast Na^{+} channel activation, and Ca^{++} accumulation and depletion are included, repectively in ν_{acc} and ν_{dep}. Deactivation is embedded in the functional timing of the in-place activation functions and the corresponding conductances. Equations (1) through (4) can mimic a wide range of neuronal dynamics, and the variables and parameters in the model represent quantities of physiological relevance for the real neuron. Parameter values throughout this work are presented in the Appendix: Model parameters, unless otherwise explicitly mentioned in the text. Numerical simulations were carried out applying the standard Runge-Kutta fourth order method implemented in a costum-made C^{++} code with step of integration h = 0.01.

The current I_{sr} is of particular interest in this work. It represents the slow repolarization calcium-dependent potassium current given by $I_{\mathrm{sr}} = \rho g_{\mathrm{sr}} a_{\mathrm{sr}}(V - V_{\mathrm{sr}})$, where V is the voltage across the cell membrane and V_{sr} is the equilibrium potential associated with the corresponding ion channels. These channels are critical for neuronal excitability in pacemaker neurons of the hypothalamic arcuate nucleus [31], for example, and are considered to be responsible for spike-frequency adaptation [32–36]. The conductance g_{sr} included in the current I_{sr} represents the maximum conductance associated with potassium channels activated by calcium, and is here implemented as control parameter for setting the individual neurons in different dynamical states. In Figure 1 we show how the dynamics of a single Huber-Braun neuron evolves depending on the values of g_{sr}. Starting tonic at $g_{\mathrm{sr}} = 0.20$ (all conductance values in this work have units of $\mathrm{mS/cm}^2$) with a firing rate $f = 8.11\,\mathrm{Hz}$, increasing the value of g_{sr} drops the firing rate to $f^{\mathrm{critical}} = 1.25\,\mathrm{Hz}$ at the transition point $g_{\mathrm{sr}}^{\mathrm{critical}} = 0.305$, where the neuron changes its firing regime from tonic to bursting.

Past $g_{\mathrm{sr}}^{\mathrm{critical}}$, now in the bursting regime, the firing rate increases to $2.125\,\mathrm{Hz}$ at $g_{\mathrm{sr}} = 0.3125$ and then starts dropping again for increasing g_{sr}. This transition in the behavior of the neuron at $g_{\mathrm{sr}}^{\mathrm{critical}}$ from tonic to bursting has been shown to influence the final state in which pairs of distinct (one tonic and the other bursting) coupled neurons synchronize [22]. Here we investigate how this intrinsic feature of the single neuron mediates a similar transition in the case of a triad of neurons electrically coupled in a linear chain format. The individual neurons are set to operate mostly in stable limit cycles but still displaying a wide variety of patterns as a function of the slow repolarization conductance g_{sr}.

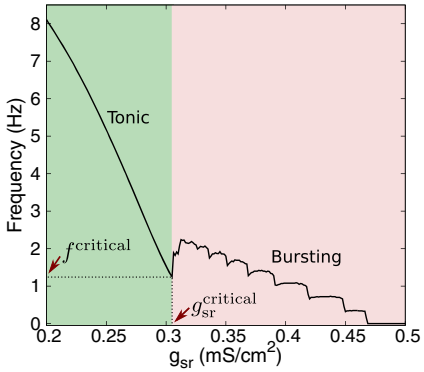

Fig. 1. Single neuron firing rate dynamics with $I_{\text{inj}} = 1.0$. For increasing g_{sr} values the single neuron firing rate decreases reaching a critical point at $g_{\text{sr}}^{\text{critical}} = 0.305$ and $f^{\text{critical}} = 1.25\,\text{Hz}$ when the neuron undergoes a tonic-to-bursting transition. The dashed vertical line indicates the boundary between tonic and bursting behaviours.

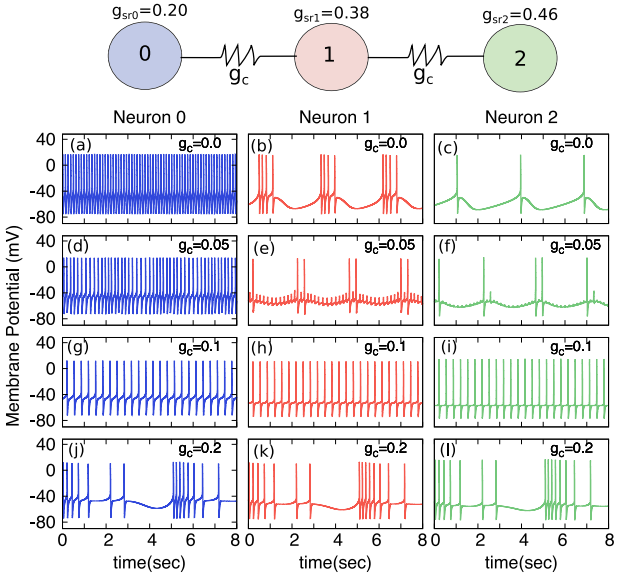

Fig. 2. Top: Schematic of three distinct coupled neurons in a linear array. Voltage vs. time for $g_c = 0.0$ (uncoupled neurons) (a) neuron 0, tonic, (b) neuron 1, bursting with four spikes per burst and (c) neuron 2, bursting with one spike per burst; for $g_c = 0.05$ (weak coupling) (d), (e), (f) the neurons change their dynamics in response to the inputs they receive from each other, but still have distinct behaviors; for $g_c = 0.1$ (stronger coupling) (g), (h), (i) the three coupled neurons synchronize in the tonic regime; for $g_c = 0.2$ (even stronger coupling) (j), (k), (l) the three neurons continue synchronized but in a different regime (chaos).

3 Linear array of coupled neurons

The network of neurons in this study consists of three distinct neurons coupled in a linear chain format, with reciprocal electrical synapses coupling the middle neuron 1 to the outer neurons 0 and 2, as illustrated in Figure 2, top. The strength of the synapses (g_c) is varied but the strength values remain identical to each other at all times in all cases discussed here. We start with neuron 0 tonic and neurons 1

and 2 bursting, with slow repolarization conductance values $g_{\mathrm{sr0}} = 0.20$, $g_{\mathrm{sr1}} = 0.38$, and $g_{\mathrm{sr2}} = 0.46$, as indicated. Voltage traces *vs.* time plots are displayed in Figures 2a, 2b and 2c in the case where the three neurons are firing independently, with $g_c = 0$.

Turning the coupling on and increasing it slightly to $g_c = 0.05$ begins to alter the dynamics of the individual neurons, as displayed by their voltage traces in Figures 2d, 2e and 2f, showing neuron 0 slowing down its firing rate while neurons 1 and 2 attempt to spike more, in a trend to increase their firing rates. Further increase in g_c eventually brings the three neurons into synchrony, with the synchronous state dependent on the strength of the coupling. For $g_c = 0.1$ the neurons synchronize in the tonic regime (Figs. 2g, 2h and 2i), and further increase to $g_c = 0.2$ synchronizes them in a bursting chaotic regime (Figs. 2j, 2k and 2l).

Next we examine three cases for the evolution of the state of the network with different individual neuronal dynamics, along with a varying coupling strength g_c. In all three cases, neuron 1 with $g_{\mathrm{sr1}} = 0.38$ and neuron 2 with $g_{\mathrm{sr2}} = 0.46$ are kept fixed. In *case 1* we set neuron 0 to $g_{\mathrm{sr0}} = 0.20$, and calculate for each neuron both the average frequency and the interspike interval for increasing values of the coupling.

Figure 3a displays the average firing rates for each neuron starting with $g_c = 0$, and increasing all the way up to $g_c = 0.3$, showing the initial firing rates of neuron 0 at $f_0 = 8.1\,\mathrm{Hz}$, of neuron 1 at $f_1 = 1.4\,\mathrm{Hz}$ and of neuron 2 at $f_2 = 0.4\,\mathrm{Hz}$. Increasing g_c values changes the firing rates of the neurons showing an overall trend for the frequencies to coalesce, approaching a common value reached when $g_c = 0.07$, where the three neurons synchronize at a firing rate $f_{sync} = 3.9\,\mathrm{Hz}$. Further increase in g_c maintains the three neurons synchronous but at various dynamical states, depending on the value of g_c. On the lower range of g_c, where the three neurons remain asynchronous, increasing g_c slows down the frequency of neuron 0 while the frequencies of neurons 1 and 2 increase up to the point where the three neurons synchronize ($g_c = 0.07$). From $g_c = 0.07$ on, increasing g_c values keeps the three neurons in synchrony, but their common firing rate decreases continuously until $g_c = 0.176$ from which point, increasing g_c on does not significantly alter the common firing rate. In Figure 3b we show a bifurcation diagram for the same three neurons and same g_c range as in Figure 3a, but now plotting the interspike intervals, not the average frequencies. Figure 3b gives us the dynamics of the three neurons for a range of g_c, and in conjunction with Figure 3a provides a more complete view of the state of not only the individual neurons but also of the state of the network as a whole. The three neurons first synchronize at $g_c = 0.07$, start a period-doubling cascade at $g_c = 0.168$ with a common firing rate which happens to be $f^{critical} = 1.25\,\mathrm{Hz}$, transitioning to chaos at $g_c = 0.176$. Continued increase of g_c leads the neurons back to periodicity with a backward bifurcation starting at $g_c = 0.255$ and into bursting at $g_c = 0.261$. This tonic-to-bursting transition has been observed for the single neuron [23] as well as for pairs of coupled neurons [22], associated with the intrinsic properties of the single neuron in its transition from tonic to bursting.

In *case 2* we set $g_{\mathrm{sr0}} = 0.23$ keeping $g_{\mathrm{sr1}} = 0.38$ and $g_{\mathrm{sr2}} = 0.46$, with the corresponding frequency and interspike interval bifurcation diagrams shown in Figures 3c and 3d, respectively. Neuron 0 now starts at a lower firing rate, 6.5 Hz, with neurons 1 and 2 starting at the same frequencies as in *case 1* above. Additionally, the three neurons first synchronize at about the same coupling strength $g_c = 0.068$ as in *case 1*, also in the tonic regime. However, the g_c range in which they remain tonic is considerably less compared to the g_c range of *case 1*. In *case 2* the synchronous neurons undergo a period-doubling bifurcation in the same manner they do in *case 1*, but in *case 2* the bifurcation happens for $g_c = 0.095$ as opposed to *case 1* where it happens for $g_c = 0.168$. This is so possibly because, compared to *case 1*, in *case 2* the dynamics of neuron 0 is closer to the dynamics of the other two neurons, therefore requiring a less strong coupling to get the three neurons in synchrony. However, the first bifurcation

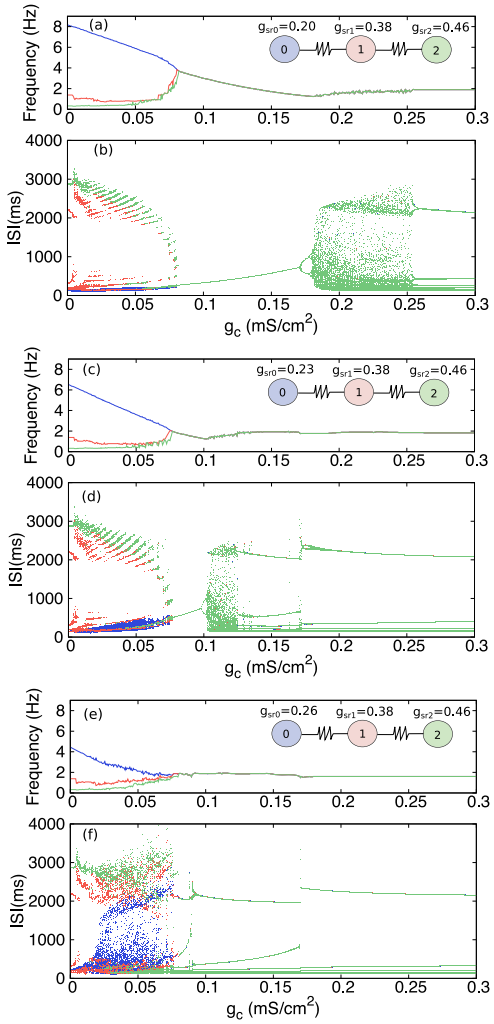

Fig. 3. Plots of frequencies (a) and interspike intervals (b) as the coupling strength increases for three distinct coupled neurons (neuron 0, tonic $g_{sr0} = 0.20$ (blue), neuron 1, bursting $g_{sr1} = 0.38$ (red) and neuron 2 bursting $g_{sr2} = 0.46$ (green)). Their dynamical states evolve to synchrony in the tonic regime for $g_c = 0.0850$. Further increase in g_c leads the three synchronous neurons into a period-doubling cascade at $g_c = 0.17$, to chaos, and to bursting starting at $g_c = 0.26$. Changing neuron 0 slow repolarization conductance to $g_{sr0} = 0.23$ and keeping neurons 1 and 2 the same, the frequencies (c) and interspike intervals (d) are shown as the coupling strength increases for the three neurons. Here also the neurons evolve to synchrony around $g_c = 0.0800$ and display a period-doubling cascade, now with a reduced coupling strength $g_c = 0.095$ and goes to the bursting at $g_c = 0.17$. Increasing the neuron 0 slow repolarization conductance to $g_{sr0} = 0.26$ and keeping neuron 1 and neuron 2 the same, the frequencies (e) and interspike intervals (f) are shown as the coupling strength increases, now with the neurons evolving into synchrony around $g_c = 0.0850$ directly into the bursting regime.

observed in *case 2* also happens for the three synchronous neurons firing at the same $f^{critical} = 1.25\,\text{Hz}$. Inside the synchronous chaotic region of Figures 3b and 3d there are several periodic windows opened by a saddle-node bifurcation and closed by a

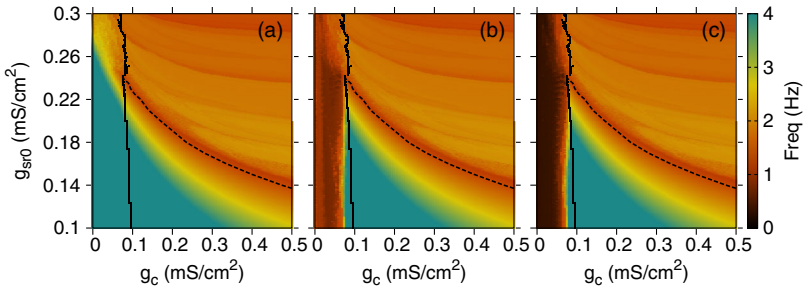

Fig. 4. Colormap showing the changes in frequencies of neuron 0 (a), neuron 1 (b) and neuron 2 (c), for varying g_{sr0} (neuron 0) values in the range [0.10:0.30] and increasing coupling strength. In this case neuron 1 and neuron 2 were kept fixed with $g_{sr1} = 0.38$ (bursting, Freq ≈ 1.5 Hz) and $g_{sr2} = 0.46$ (bursting, Freq ≈ 0.4 Hz). The black solid line indicates the coupling strength at which the three neurons synchronize and the dashed line depicts the first period-doubling in the period-doubling cascade.

global bifurcation, typical of an interior crisis [37,38]. Also, reference [39] discusses the mechanisms of tonic-to-bursting transition in single neurons via Hopf bifurcation.

For $g_{\mathrm{sr0}} = 0.26$ in *case 3*, the frequency and bifurcation diagrams displayed in Figures 3e and 3f, respectively, show that the three neurons synchronize at $g_c = 0.07$, with a frequency $f = 1.95$ Hz directly into the bursting regime, forgoing the period-doubling cascade and chaos transition observed in *cases 1* and *2*. Figures 3e and 3f further show that the synchronous frequency of the three neurons remains about constant in the range of g_c between 0.07 and 0.3 (Fig. 3e) even though their bursting dynamics changes within this same g_c range (Fig. 3f).

4 Frequency dynamics

To further investigate the interactions between tonic and bursting networked neurons we expand the range of g_{sr} for one of the neurons while keeping the other two fixed, in three different scenarios. The aim here is to verify the extent of the tonic-bursting transition displayed by the synchronous neurons in parameter space of g_c and the three g_{sr}'s. In *scenario 1*, we vary g_{sr0} in the [0.1:0.3] range (keeping neuron 0 tonic), and fix $g_{\mathrm{sr1}} = 0.38$ and $g_{\mathrm{sr2}} = 0.46$, both bursting. Figure 4 shows three maps with the neurons' firing rates color coded according to the palette on the right-hand side. On the x-axis of the maps we have the coupling strength g_c and on the y-axis we have g_{sr0}. The colors displayed on the maps of Figures 4a, 4b and 4c correspond to the firing rates of neurons 0, 1 and 2, respectively. On each map, the black continuous approximately vertical line indicates the minimum g_c values for which the neurons synchronize. On the right-hand side of the black line, the colors represent the firing rates of the individual *synchronous* neurons, and therefore the three color maps on the right-hand side of the black line are identical. On the left-hand side of the black line, the neurons are *non-synchronous*, so the color maps in this case are different.

The black dashed curved lines in Figure 4 indicate g_c values for which the synchronous neurons undergo the first period-doubling bifurcation. This line falls on the left border of a strip (red) of lower firing rate compared to the surrounding areas (orange) on both sides. The firing rate on this strip matches the $f^{\mathrm{critical}} = 1.25$ Hz for the single neuron illustrated in Figure 1, and the width of the strip corresponds to the range of g_c for the length of the period-doubling bifurcation cascade, up to the point where the system reaches chaos. Immediately to the left of the red strip the neurons are synchronized in the tonic regime, and to the right of the red

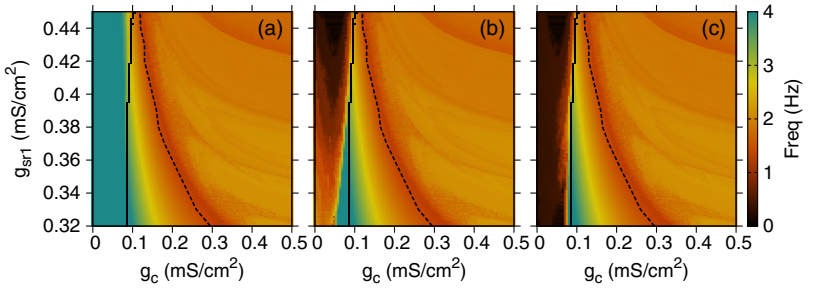

Fig. 5. Colormap showing the changes in frequencies of neuron 0 (a), neuron 1 (b) and neuron 2 (c), for varying g_{sr1} (neuron 1) values in the range [0.32:0.45] and increasing coupling strength. In this case neuron 0 and neuron 2 were kept fixed with $g_{sr0} = 0.20$ (tonic, Freq ≈ 8.0 Hz) and $g_{sr2} = 0.46$ (bursting, Freq ≈ 0.4 Hz). The black solid line indicates the coupling strength at which the three neurons synchronize and the dashed line depicts the first period-doubling in the period-doubling cascade.

strip the neurons are synchronized in the bursting regime. The strip therefore represents a parameter space region for which the transition between tonic and bursting regimes is mediated by a period-doubling bifurcation cascade (width of the strip) followed by chaos. Two specific examples are shown in the bifurcation diagrams of Figures 3b and 3d, where the first period-doubling bifurcation point in the bifurcation diagrams correspond to points of minima in the frequency bifurcation diagrams of Figures 3a and 3c. In the color maps of Figures 4a, 4b and 4c, the point where the black continuous line and the black dashed line intersect marks the maximum $g_{\mathrm{sr0}}^{\mathrm{max}} = 0.24$ for which a period-doubling cascade exists in this configuration. Neuron 0 with $g_{\mathrm{sr}} > g_{\mathrm{sr0}}^{\mathrm{max}}$ will display no period-doubling cascade in the tonic-bursting transition, as shown in the specific example of Figure 3f where $g_{\mathrm{sr0}} = 0.26$.

In *scenario 2* we maintain the same tonic-bursting-bursting setting for the three-neuron network, but now we change the dynamics of neuron 1, with g_1 varying in the [0.32:0.45] range (keeping neuron 1 bursting). The frequency color maps for the three neurons are shown in Figures 5a, 5b and 5c for neurons 0, 1, and 2, respectively. As in *scenario 1*, the continuous black line represents minimum g_c values for synchronization and the dashed black line represents g_c values for the first period doubling bifurcation point. Here too, the black dashed line follows a strip (red) of lower firing rate compared to the surrounding areas (yellow) on both sides. However, in this range of g_{sr1} the continuous and the dashed lines to not intersect and all bifurcation diagrams in this configuration exhibit period doubling cascades.

Finally, in *scenario 3* we follow the same setup of the two previous scenarios, but here we change the dynamics of neuron 2, varying g_{sr2} in the [0.45:0.50] range (keeping neuron 2 bursting). In this scenario neurons 1 and 2 remain more similar to each other and more different from neuron 0, with the color map of Figure 6a being more different than the two more similar color maps of Figures 6b and 6c. The continuous and dashed black lines in this scenario are positioned in a more parallel disposition, distinctly separated, indicating that while there will always be a period doubling cascade in the bifurcation diagrams, the transition between non-synchronous and synchronous states will never happen with the synchrony in the typical tonic period-one state. Even though the scenarios described above correspond to different ranges of g_{sr} for the neurons, all three scenarios share the common feature of first synchrony happening for $g_c \approx 0.07$. Moreover, the transition between tonic and bursting synchronous states happens with the three neurons sharing the common firing rate $f = 1.25$ Hz, which corresponds to the f^{critical} displayed by the single neuron when transitioning between tonic and bursting regimes, shown in Figure 1.

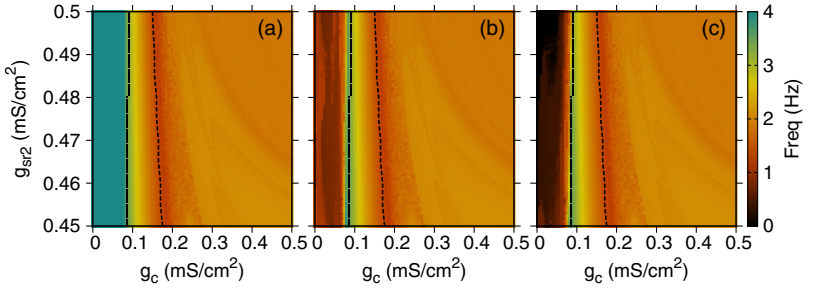

Fig. 6. Colormap showing the changes in frequencies of neuron 0 (a), neuron 1 (b) and neuron 2 (c), for varying neuron 2 g_{sr2} values in the range [0.45 : 0.50] and increasing coupling strength. In this case neuron 0 and neuron 1 were kept fixed with $g_{sr0} = 0.2$ (tonic, Freq ≈ 8 Hz) and $g_{sr1} = 0.38$ (bursting, Freq ≈ 1.5 Hz). The black solid line indicates the coupling strength the three neurons synchronize and the dashed line depicts the first period-doubling in the period-doubling cascade.

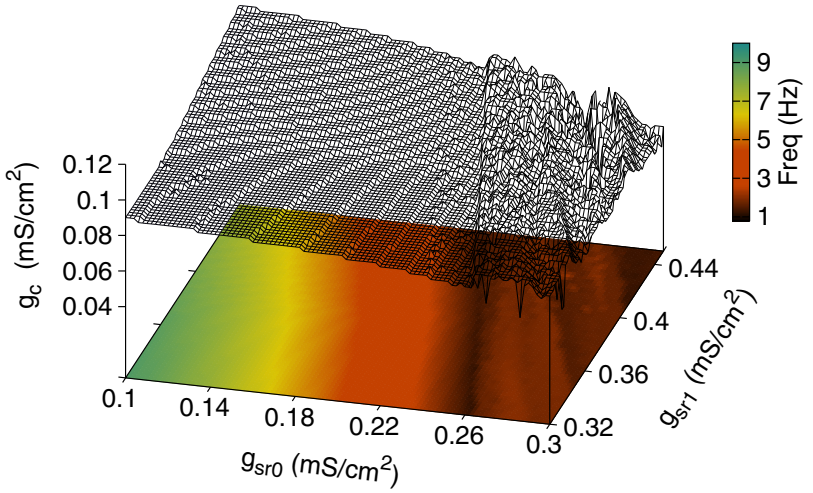

Fig. 7. Four-dimensional plot showing the combined changes of the tonic neuron 0 (g_{sr0}) and the bursting neuron 1 (g_{sr1}). Neuron 2 was kept constant at $g_{sr2} = 0.46$, bursting. The z-axis shows the coupling strength in which the three neurons synchronize. Color shows the frequency in which the three neurons synchronize.

This feature of coupled synchronous neurons, in their transition between tonic and bursting states, displaying the very same f^{critical} as the single neuron, has been observed before in the case of pairs of neurons [22]. Here we show that the carrying over of this single neuron intrinsic property also happens in a more general setting, with three coupled neurons in a wide range of g_{sr} values.

A more comprehensive representation of the network dynamics is depicted in the four-dimensional plot of Figure 7, where the range of g_{sr0} is set at [0.1:0.3] (tonic), and of g_{sr1} at [0.32:0.44] (bursting). The value of is kept constant at $g_{\text{sr2}} = 0.46$ (bursting). The colors represent the firing rates of the neurons upon synchronization according to the color palette on the right-hand side, and the mesh displays along the z-axis the values of the minimum coupling strength g_c for which the three neurons synchronize. The g_{sr0} *vs.* g_{sr1} color plate shows that the firing rate at which the neurons synchronize decreases for increasing g_{sr0} and g_{sr1} values.

Also, the dark stripe observed in this color plane, starting at (g_{sr0}, g_{sr1}) point (0.26, 0.32) and ending at point (0.22, 0.44) following a negative slope, corresponds to the bump observed on the mesh separating the plateau-like surface on the left-hand side (tonic first synchronization) from the bumpy surface on the right-hand side (bursting, first synchronization). The firing rate of the neurons in the configurations corresponding to points along the dark stripe (border between tonic and bursting first synchronization) equals the $f^{\mathrm{critical}} = 1.25\,\mathrm{Hz}$ of the single neuron in its transition between tonic and bursting regimes, as illustrated in Figure 1. This indicates that the intrinsic characteristic f^{critical} of the individual neurons plays a specific role in their synchronization process, remarkably, when they undergo a transition from tonic firing to bursting in their synchronized states.

5 Conclusion

Neuronal synchronization is relevant for the proper functioning of many neuronal circuits and vital for the continuation of more than a few species. There are many important aspects associated with synchronous neurons including, and of major interest in this work, transitions between tonic and bursting states. We address this issue using triads of model neurons reciprocally coupled via electrical synapses in a linear chain format. Our single model neuron equations [25] display fast and slow repolarization and depolarization currents, eliciting slow subthreshold voltage oscillations typical of bursting activity. A firing rate characteristic of this single neuron transition between tonic and bursting behaviors (Fig. 1) is here shown to be also found in the case of an equivalent transition for the triad of coupled neurons. The set of three neurons consists of one neuron tonic (neuron 0) and the other two bursting (neuron 1 with multiple spikes per burst, and neuron 2 with one spike per burst), as illustrated in Figure 2, with the dynamics of the network being studied with respect to two important parameters: the slow repolarization conductance g_{sr} for the individual neurons, and the neuronal coupling strength g_c between pairs of neurons.

Initially, we analyse three cases in which the g_{sr} values of the two bursting neurons are held constant while the tonic neuron's g_{sr0} is varied (Fig. 3). We found that the three coupled neurons synchronize at a rather small and approximately constant coupling strength, regardless of g_{sr0} value assigned to the tonic neuron. After synchronization, however, different bifurcation structures are observed for continued increase of the coupling strength. In the first case, for $g_{\mathrm{sr0}} = 0.20$ (Fig. 3b), the three neurons first synchronize in a tonic (period-one) regime followed by a period doubling cascade taking place at $g_c = 0.17$, followed by chaos and then bursting. Similar sequence is observed for $g_{\mathrm{sr0}} = 0.23$ (Fig. 3d), but now the period doubling cascade happens at $g_c = 0.095$, substantially decreasing the g_c range for the period-one synchronous state. As in the previous case, chaos and bursting follow the period doubling cascade. Further increase of the g_{sr0} value to 0.26 (Fig. 3f) leads the three neurons to first synchronize in the bursting regime, bypassing the transition observed in the previous two cases. The feature to be noted in these three cases is in regards to the change observed in the state of the neurons when they first synchronize, either tonic (*case 1* and *case 2*) or bursting *case 3*. However, the characteristic firing rate $f^{critical} = 1.25\,\mathrm{Hz}$ is present only in the first two cases, where the existing tonic-to-bursting transition is mediated by the period-doubling cascade and chaos.

To further explore the connection between the transition observed in the single neuron and the corresponding transition encountered in the networked neurons we set neuron 2 fixed and vary neurons 0 and 1 as denoted in Figure 7. The color map shows the typical decrease in firing rate for increasing g_{sr} values for both neuron 0 and neuron 1. Additionally, the color map shows a dark stripe with negative slope

in the g_{sr0} *vs.* g_{sr1} plane. This stripe separates regions of tonic (to the left) and of bursting (to the right) synchronous behaviors for the three neurons. The distinction between these two regions is more visible in the mesh with the same g_{sr0} *vs.* g_{sr1} coordinates but with the coupling strength g_c as third coordinate. This mesh shows a sharp transition above the same region where the dark stripe is located in the color map. Most interestingly, the value of the firing rate along this stripe is the same $f^{critical} = 1.25\,\mathrm{Hz}$ encountered in the single neuron tonic-to-bursting transition.

For future investigation of this unique phenomenon we expect the characteristic firing rate $f^{critical}$ of the single neuron to be carried over in the case of networks more complex than the triads studied here, including the case of bursting neuron models other than the Huber-Braun presently used.

Appendix A: Model parameters

$g_{\mathrm{leak}} = 0.1$ mS/cm^2, $V_{\mathrm{leak}} = -60$ mV, $I_{\mathrm{syn}} = 1.0$ μA/cm^2
$g_{\mathrm{Na}} = 1.5$ mS/cm^2, $V_{\mathrm{Na}} = 50$ mV, $V_{0\mathrm{Na}} = -25$ mV
$g_{\mathrm{K}} = 2.0$ mS/cm^2, $V_{\mathrm{K}} = -90$ mV, $V_{0\mathrm{K}} = -25$ mV
$g_{\mathrm{sd}} = .25$ mS/cm^2, $V_{\mathrm{sd}} = 50$ mV, $V_{0\mathrm{sd}} = -40$ mV
$g_{\mathrm{sr}} = .25$ mS/cm^2, $V_{\mathrm{sr}} = -90$ mV, $C = 1$ μF/cm^2
$\tau_{\mathrm{K}} = 2.0$ ms, $\tau_{\mathrm{sd}} = 10.0$ ms, $\tau_{\mathrm{sr}} = 20.0$ ms
$s_{\mathrm{K}} = 0.25$ mV^{-1}, $s_{\mathrm{sd}} = 0.09$ mV^{-1}, $s_{\mathrm{sNa}} = 0.25$ mV^{-1}
$\rho = 0.607$, $\phi = 0.124$, $\nu_{\mathrm{acc}} = 0.17$, $\nu_{\mathrm{dep}} = 0.012$

References

1. E.K. Miller, T.J. Buschman, Cortical circuits for the control of attention, Curr. Opin. Neurobiol. **23**, 216 (2013)
2. R. Follmann, E.E.N. Macau, E. Rosa, J.R.C. Piqueira, Phase oscillatory network and visual pattern recognition, IEEE Trans. Neural Netw. Learn. Syst. **26**, 1539 (2015)
3. S. Horvát, R. Gămănu, M. Ercsey-Ravasz, L. Magrou, B. Gămănu, D.C. Van Essen, A. Burkhalter, K. Knoblauch, Z. Toroczkai, H. Kennedy, Spatial embedding and wiring cost constrain the functional layout of the cortical network of rodents and primates, PLoS Biol. **14**, e1002512 (2016)
4. S. Daan, D.G. Beersma, A.A. Borbély. Timing of human sleep: Recovery process gated by a circadian pacemaker, Am. J. Physiol. Regul. Integr. Comp. Phys. **246**, R161 (1984)
5. S. Postnova, K. Voigt, H.A. Braun, Neural synchronization at tonic-to-bursting transitions, J. Biol. Phys. **33**, 129 (2007)
6. E. Marder, D. Bucher, Central pattern generators and the control of rhythmic movements, Curr. Biol. **11**, R986 (2001)
7. W. Van Drongelen, H. Koch, C. Marcuccilli, F. Pena, J. Ramirez, Synchrony levels during evoked seizure-like bursts in mouse neocortical slices, J. Neurophysiol. **90**, 1571 (2003)
8. F. Mormann, T. Kreuz, R.G. Andrzejak, P. David, K. Lehnertz, C.E. Elger, Epileptic seizures are preceded by a decrease in synchronization, Epilepsy Res. **53**, 173 (2003)
9. C. Hammond, H. Bergman, P. Brown. Pathological synchronization in parkinson's disease: networks, models and treatments, Trends Neurosci. **30**, 357 (2007)
10. E.J. Furshpan, D.D. Potter, Mechanism of nerve-impulse transmission at a crayfish synapse, Nature **180**, 342 (1957)
11. E. Marder, G. Gutierrez, M.P. Nusbaum, Complicating connectomes: Electrical coupling creates parallel pathways and degenerate circuit mechanisms, Dev. Neurobiol. **77**, 597 (2017)

12. M. Galarreta, S. Hestrin, Electrical and chemical synapses among parvalbumin fast-spiking gabaergic interneurons in adult mouse neocortex, Proc. Natl. Acad. Sci. **99**, 12438 (2002)
13. P.L. Carlen, F. Skinner, L. Zhang, C. Naus, M. Kushnir, J.L. Perez Velazquez, The role of gap junctions in seizures, Brain Res. Rev. **32**, 235 (2000)
14. M.VL. Bennett, R.S. Zukin, Electrical coupling and neuronal synchronization in the mammalian brain, Neuron. **41**, 495 (2004)
15. N.P. Franks, General anaesthesia: from molecular targets to neuronal pathways of sleep and arousal, Nat. Rev. Neurosci. **9**, 370 (2008)
16. Y.B. Saalmann, S. Kastner, Gain control in the visual thalamus during perception and cognition, Curr. Opin. Neurobiol. **19**, 408 (2009)
17. S. Bahar, Burst-enhanced synchronization in an array of noisy coupled neurons, Fluctuation Noise Lett. **4**, L87 (2004)
18. S.M. Sherman, Tonic and burst firing: Dual modes of thalamocortical relay, Trends Neurosci. **24**, 122 (2001)
19. R.R. Llinás, M. Steriade, Bursting of thalamic neurons and states of vigilance, J. Neurophysiol. **95**, 3297 (2006)
20. A. Shilnikov, G. Cymbalyuk, Transition between tonic spiking and bursting in a neuron model via the blue-sky catastrophe, Phys. Rev. Lett. **94**, 048101 (2005)
21. F. Fröhlich, M. Bazhenov, Coexistence of tonic firing and bursting in cortical neurons, Phys. Rev. E **74**, 031922 (2006)
22. A. Shaffer, A.L. Harris, R. Follmann, E. Rosa, Bifurcation transitions in gap-junction-coupled neurons, Phys. Rev. E **94**, 042301 (2016)
23. S. Postnova, B. Wollweber, K. Voigt, H. Braun, Impulse pattern in bi-directionally coupled model neurons of different dynamics, BioSyst. **89**, 135 (2007)
24. A.L. Hodgkin, A.F. Huxley, A quantitative description of membrane current and its application to conduction and excitation in nerve, J. Physiol. **117**, 500 (1952)
25. R. Gilmore, X. Pei, F. Moss, Topological analysis of chaos in neural spike train bursts, Chaos: An Interdiscip. J. Nonlinear Sci. **9**, 812 (1999)
26. M.T. Huber, H.A. Braun, Conductance versus current noise in a neuronal model for noisy subthreshold oscillations and related spike generation, Biosyst. **89**, 38 (2007)
27. S. Postnova, E. Rosa, H.A. Braun, Neurones and synapses for systemic models of psychiatric disorders, Pharmacopsychiatry **43**, S82 (2010)
28. C. Finke, J.A. Freund, E. Rosa Jr, P.H. Bryant, H.A. Braun, U. Feudel, Temperature-dependent stochastic dynamics of the huber-braun neuron model, Chaos: An Interdiscip. J. Nonlinear Sci. **21**, 047510 (2011)
29. S. Postnova, P.A. Robinson, D.D. Postnov, Adaptation to shift work: Physiologically based modeling of the effects of lighting and shifts start time, PloS One **8**, e53379 (2013)
30. E. Rosa, Q.M. Skilling, W. Stein, Effects of reciprocal inhibitory coupling in model neurons, Biosyst. **127**, 73 (2015)
31. M. van den Top, K. Lee, A.D. Whyment, A.M. Blanks, D. Spanswick, Orexigen-sensitive npy/agrp pacemaker neurons in the hypothalamic arcuate nucleus, Nat. Neurosci. **7**, 493 (2004)
32. P. Sah, Ca^{2+}-activated K^+ currents in neurones: Types, physiological roles and modulation, Trends Neurosci. **19**, 150 (1996)
33. C. Vergara, R. Latorre, N.V. Marrion, J.P. Adelman, Calcium-activated potassium channels, Curr. Opin. Neurobiol. **8**, 321 (1998)
34. B. Ermentrout, M. Pascal, B. Gutkin, The effects of spike frequency adaptation and negative feedback on the synchronization of neural oscillators, Neural Comput. **13**, 1285 (2001)
35. J. Benda, A. Longtin, L. Maler, Spike-frequency adaptation separates transient communication signals from background oscillations, J. Neurosci. **25**, 2312 (2005)
36. J.P. Roach, L.M. Sander, M.R. Zochowski, Memory recall and spike-frequency adaptation, Phys. Rev. E **93**, 052307 (2016)

37. U. Feudel, A. Neiman, X. Pei, W. Wojtenek, H. Braun, M. Huber, F. Moss, Homoclinic bifurcation in a Hodgkin-Huxley model of thermally sensitive neurons, Chaos: An Interdiscipl. J. Nonlinear Sci. **10**, 231 (2000)
38. W. Braun, B. Eckhardt, H.A. Braun, M. Huber, Phase-space structure of a thermoreceptor, Phys. Rev. E **62**, 6352 (2000)
39. O.V. Sosnovtseva, S.D. Postnova, E. Mosekilde, H.A. Braun, Inter-pattern transitions in a noisy bursting cell, Fluctuation Noise Lett. **4**, L521 (2004)